

Competition of Failure Modes under In-Phase and Out-of-Phase loading in a gear steel

S. Beretta, S. Foletti, K. Valiullin

Politecnico di Milano, Dept. Mechanical Eng., Via La Masa 34, 20156 Milano.

e-mail: stefano.beretta@polimi.it, stefano.foletti@polimi.it, khaydar.valiullin@polimi.it

ABSTRACT. *In order to investigate the fatigue crack propagation under Mode III, torsional fatigue tests which use shallow micro notches on a SAE 5135 gear steel were carried out. The initial small cracks were introduced by a preliminary Mode I fatigue test pre-cracking, in order to promote co-planar crack propagation using the specimens with the artificial defect. Torsion fatigue tests for a shallow micro defects showed that starting from the $\sqrt{\text{area}}$ of micro defects equal to the $221.2 \mu\text{m}$ it was possible to obtain stable co-planar fatigue crack growth in Mode III, at stress levels slightly higher than the Mode I threshold $\Delta K_{th,I}$. Moreover, in order to investigate the crack path under mixed mode loading, some in-phase and out-of-phase axial torsion fatigue tests were carried out. The results of the multiaxial fatigue tests with mode mixity similar to rolling contact fatigue condition show a stable co-planar growth.*

INTRODUCTION

Fatigue strength in the presence of inhomogeneities is controlled by the threshold condition of small cracks which nucleate at the defect tip. Therefore, the fatigue limit is associated with the threshold condition of small cracks [1].

Mode II and Mode III crack growth is frequently observed in mechanical components subjected to heavy repeated rolling contact loads such as rails, bearings etc. and in components transmitting torque, like rotor shafts, drive shafts. This type of crack initiation is induced by the presence of the micro defects [2].

Surface-initiated cracks in rolling contact fatigue are often submitted to a complex sequence of Mode I + Mode III loading [3]. Few studies have been devoted to describe fatigue crack propagation under non-proportional mixed Mode loading in the presence of small cracks and some results suggest that such loading might be specially damaging [4]. It has been recognized in existing literature that analyzing the path of small cracks is essential to make clear mechanical and micro structural factors affecting the fatigue strength under mixed mode loading.

The aim of the present study is to improve the understanding of the crack growth in a condition close to the one experienced by the material in the contact rolling fatigue where an out-of-phase superposition of Mode I and Mode II/Mode III can be able to sustain stable co-planar growth. Different torsional fatigue tests for shallow micro defects of different size were carried out in order to obtain a stable co-planar fatigue

crack growth, threshold in Mode III for a gear steel. Moreover, multiaxial fatigue tests were carried out on the same steel in order to investigate the effect of a superimposed compressive axial load on the stable co-planar crack growth.

EXPERIMENTAL DETAILS

Material

The material analysed is a quenched and tempered SAE 5135 steel ($\sigma_{\text{uts}}=2150$ MPa, $\sigma_y=1395$ MPa). A series of experimental tests were carried out with the purpose to characterize the basic mechanical properties and the fatigue behaviour of the material: monotonic tensile tests, cyclic strain controlled low cycle fatigue tests, high cycle axial fatigue tests on smooth specimens and on micro-notched specimens.

In Fig.1a is shown the comparison between the cyclic and the monotonic tensile curve. The material shows a hardening behaviour when subjected to cyclic loading with a cyclic 0.2% proof stress $\sigma_{y0.2\%} = 1735$ MPa.

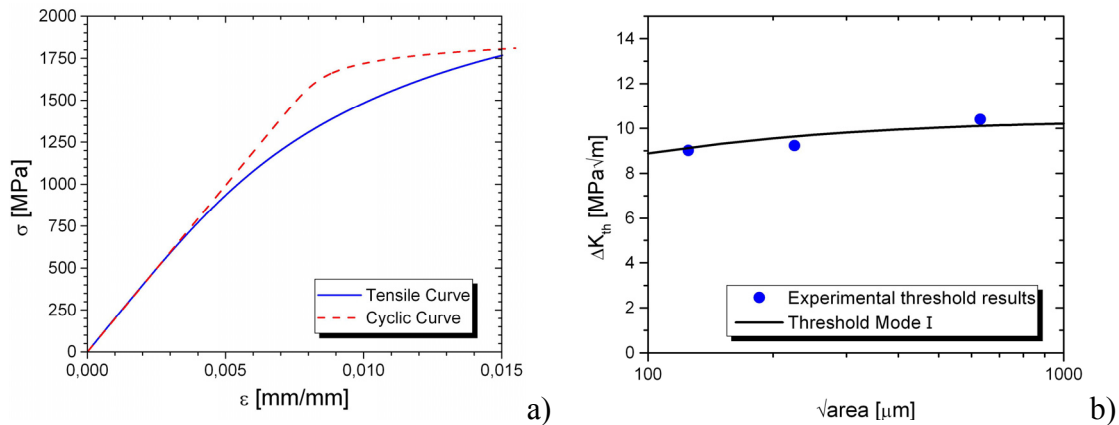


Figure 1. a) cyclic curve versus monotonic tensile curve, b) Kitagawa diagram

A series of bending fatigue test, at $R= -1$ onto micro notched and smooth specimens, in order to determine the relationship between fatigue strength and defect size, were carried out. Since it was possible to observe non-propagating cracks in the tip and bottom of the micronotch of the run out specimens, fatigue limit was associated with the thresholds of these cracks (see Fig.1b), which can be expressed as:

$$\Delta K_{\text{th}} = \Delta K_{\text{th,LC}} \cdot \sqrt{\frac{\sqrt{\text{area}}}{\sqrt{\text{area}} + \sqrt{\text{area}_0}}} \quad (1)$$

where defect/crack size is expressed in $\sqrt{\text{area}}$ parameter by Murakami [5].

Specimens for Torsion and Multiaxial Fatigue Tests

Before the starting torsional and multiaxial fatigue tests, all specimens were electro polished to avoid the effect of the surface residual stresses. Then, artificial micro

notches were introduced by means of electro-discharging machining. The geometry of the specimens and micro notches adopted are represented in Fig.2.

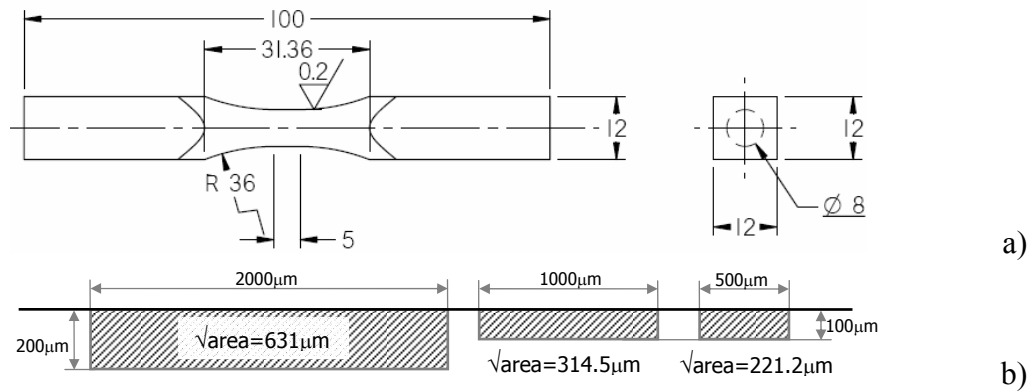


Figure 2. a) specimen shape and dimensions, b) micro notches geometry adopted for torsional and multiaxial fatigue tests

The initial small cracks were introduced by a preliminary Mode I fatigue test pre-cracking, in order to promote co-planar crack propagation. All specimens were subjected to bending fatigue for 12×10^6 cycles at $R=-2$ at a stress levels very close to $\Delta K_{th,I}$. This procedure induced small non-propagating cracks at the bottom of the notch with a depth of approximately 20 μm (see Fig.3).

The specimens underwent fatigue tests with the following procedure: i) SEM observation for verifying pre-cracking after bending tests; ii) torsional/multiaxial fatigue test; iii) SEM observation after torsional/multiaxial fatigue tests; iv) static rupture in liquid nitrogen; v) SEM observations of the fracture surface (or repeated polished sections). The cracks emanating from the shallow defects were modelled by means of finite element method, in order to correctly estimate ΔK_{III} at the tip of the non-propagating cracks.

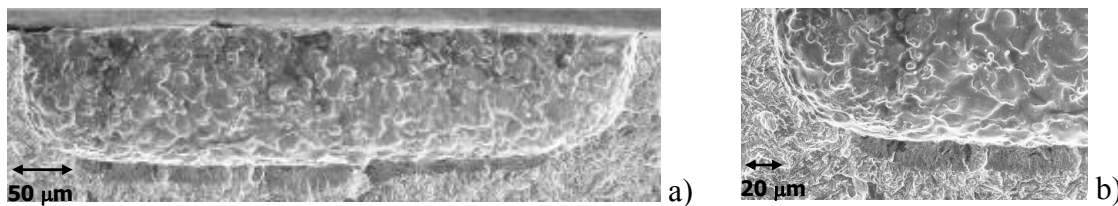


Figure 3. Non-propagating crack at the bottom of the micronotch $\sqrt{\text{area}}=221.2 \mu\text{m}$, after pre-cracking $R=-2$ for 10^7 cycles (specimen broken under liquid nitrogen)

TORSIONAL FATIGUE TESTS

Torsional fatigue tests with transverse pre-cracked micro notches were carried out at different ΔK_{III} levels.

The results of torsional fatigue tests show that at ΔK_{III} levels near $\Delta K_{th,I}$ there is formation of a semi-elliptical Mode III ‘pockets’, similar to the once observed by Murakami et al [2] at Mode III threshold (Fig.4, 5a). The conclusion that $\Delta K_{th,III}$ corresponds to ‘discontinuous’ co-planar crack is confirmed by the average da/dN measured from the cracks advance. At higher ΔK_{III} levels (for defects with $\sqrt{\text{area}}=221 \mu\text{m}$ at $\Delta K_{III}=1.08 \Delta K_{th,I}$ and at $\Delta K_{III}=1.3 \Delta K_{th,I}$ for defects with $\sqrt{\text{area}}=314.5$ and $631 \mu\text{m}$) the discontinuous co-planar growth turns into a stable crack advance (Fig. 5b, c), with growth rates around 10^{-9} m/cycle.

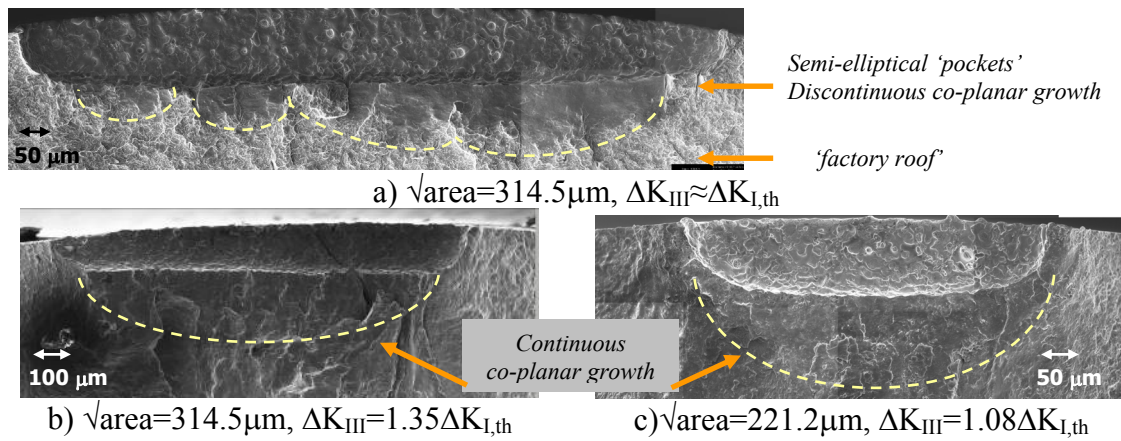


Figure 4. Fractography of torsion test co-planar growth examples a) discontinuous crack advance b), c) continuous co-planar growth

It is of some importance to note that for $\Delta K_{III} > \Delta K_{th,I}$ all the specimens failed for Mode I, on fracture planes at 45° : Mode I failures implies that growth rate under tension is higher than co-planar growth under shear. These planes corresponds to planes where there is the maximum Mode I ($\Delta K_\theta = \Delta K_{III}$ for $\theta=45^\circ$ [6]).

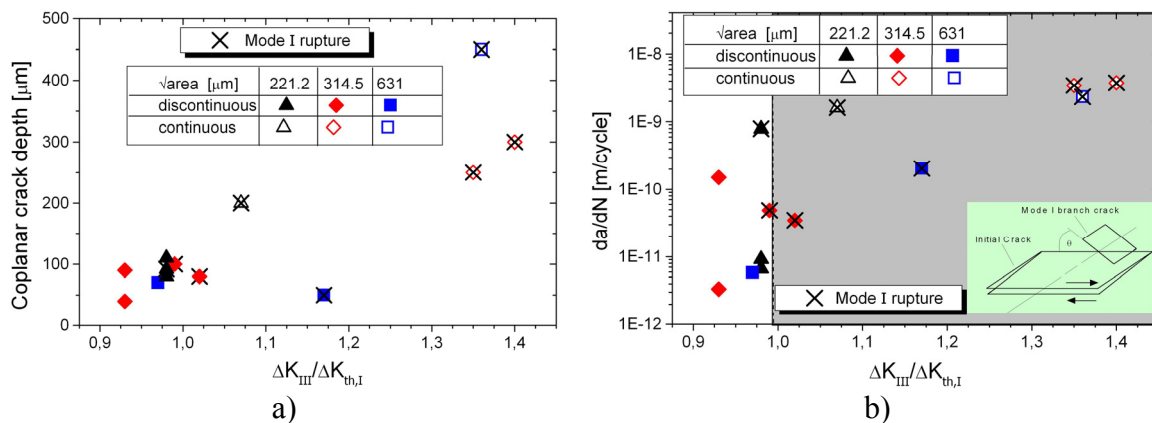


Figure 5. Torsional fatigue test results: a) co-planar crack advance vs ΔK_{III} ; b) average growth rate measured from crack advance

MULTIAXIAL FATIGUE TESTS

Biaxial fatigue tests were carried out by means of MTS 809 Axial Torsional System. Optical microscope Leica system was used to control surface crack propagation. Two general types of multiaxial fatigue tests were fulfilled: in-phase axial-torsional one at stress ratio $R=-1$, and out-of-phase torsional at $R=-1$ with axial load in compression shifted at $\delta=90^\circ$ relatively torsional phase (Fig.6). Three types of the micro notches were adopted, see Fig. 2, for multiaxial tests. All the specimens have been prepared following the same procedure described for the torsional fatigue tests.

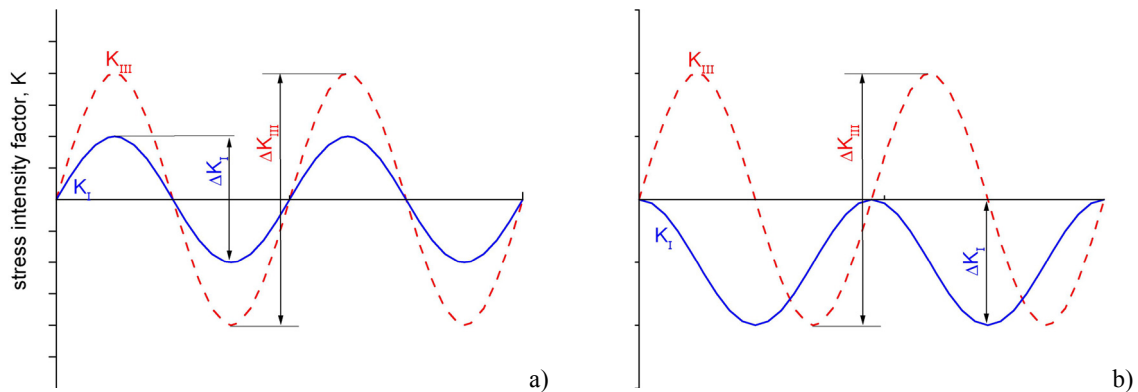


Figure 6. Multiaxial fatigue tests scheme a) in-phase and b) out-of-phase

The results of multiaxial fatigue tests are shown in the Table 1-2. In last two out-of-phase multiaxial fatigue tests (specimen O.2 and O.3) the value of the mean compressive axial stress has been increased in order to simulate the real state of stress in rolling contact fatigue problems. In fact, in pure rolling contact in the sub-surface region, where the shear stress amplitude is maximum, the ratio between the normal mean stress and shear stress amplitude is approximately equal to 1.5 [7].

Table 1. In-phase multiaxial test results

Specimen №	Micro notch $\sqrt{\text{area}} [\mu\text{m}]$	$\Delta K_{III}/\Delta K_{th,I}$	$\Delta K_I/\Delta K_{th,I}$	N [cycles]	co-planar Mode III crack depth $[\mu\text{m}]$	surface crack growth $[\mu\text{m}]$
I.1	314.5	0.60	0.35	1000000	No cracks	
I.2	314.5	0.72	0.42	500000		
I.3	314.5	1.06	0.39	159796	~ 150 discontinuous	> 2000 (failed)
I.4	314.5	0.97	0.35	65683	~ 150 discontinuous	1500
I.5	314.5	0.87	0.32	298561	no evidence	> 2000 (failed)
I.6	314.5	0.87	0.32	103765	no evidence	1500
I.7	221.2	0.85	0.31	118654	no evidence	950
I.8	221.2	0.70	0.25	221022	no evidence	970

Table 2. Out-of-phase multiaxial tests results

Specimen №	Micro notch $\sqrt{\text{area}}$ [μm]	$\Delta K_{III}/\Delta K_{th,I}$	$\Delta K_I/\Delta K_{th,I}$	N [cycles]	co-planar Mode III crack depth [μm]	surface crack growth [μm]
O.1	314.5	0.87	0.32 (-)	225550	~ 100 discontinuous	567
O.2	221.2	1.08	1.94 (-)	727744	~ 480	162
O.3	631	1.57	3.42 (-)	116866	~ 1250	550

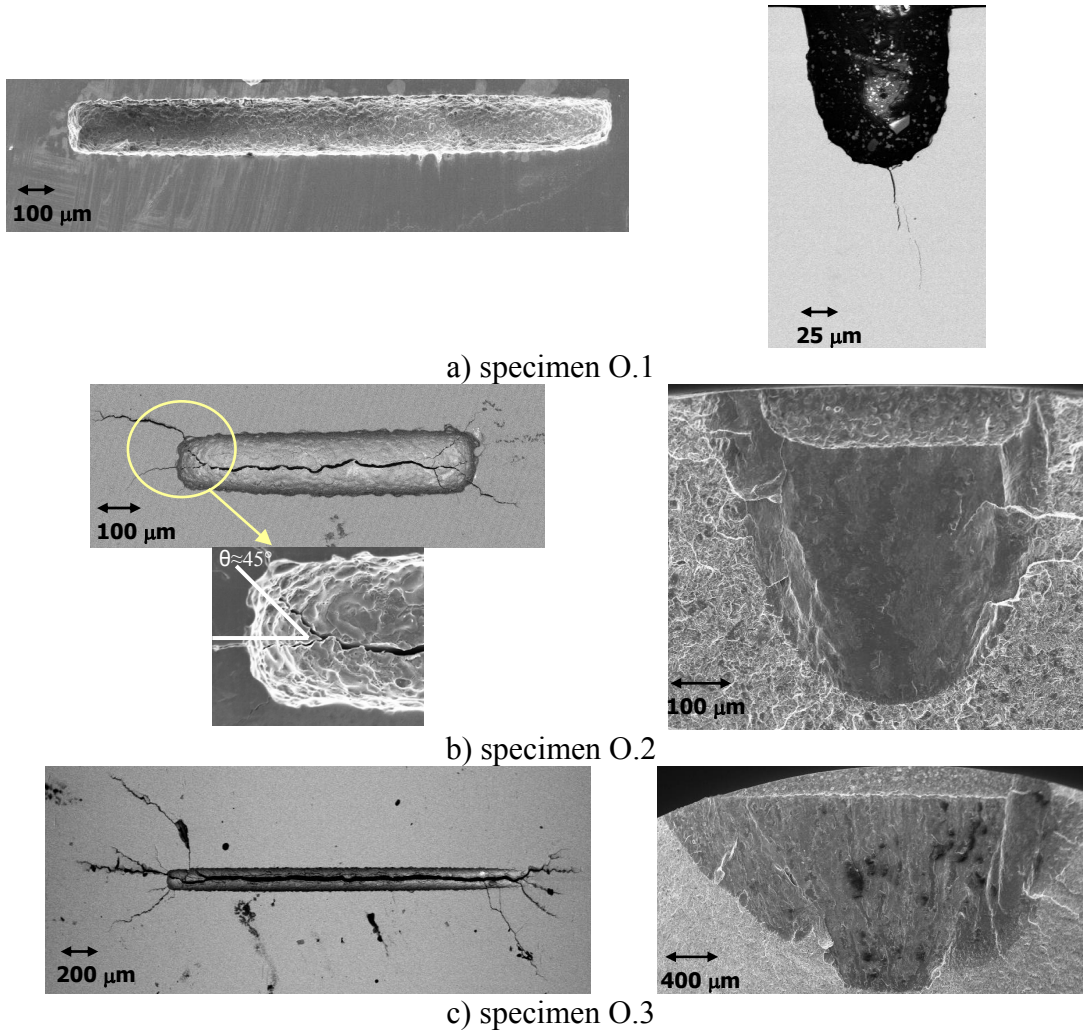


Figure 7. Fractography of multiaxial out-of-phase tests

Having a look at a very first results of the multiaxial fatigue tests (see Fig.7) is clear that the out-of-phase scheme of loading favours Mode III co-planar crack growth, instead of that in-phase tests where co-planar growth similar to the one of the torsional tests.

To estimate Mode III co-planar crack growth speed under out-of-phase loading several tests at the same stress levels were carried out on the specimens with micronotch

$\sqrt{\text{area}}=221.2 \mu\text{m}$, interrupting the test at different number of test cycles, and breaking them in liquid nitrogen to measure the depth of the crack (see Fig 8.)

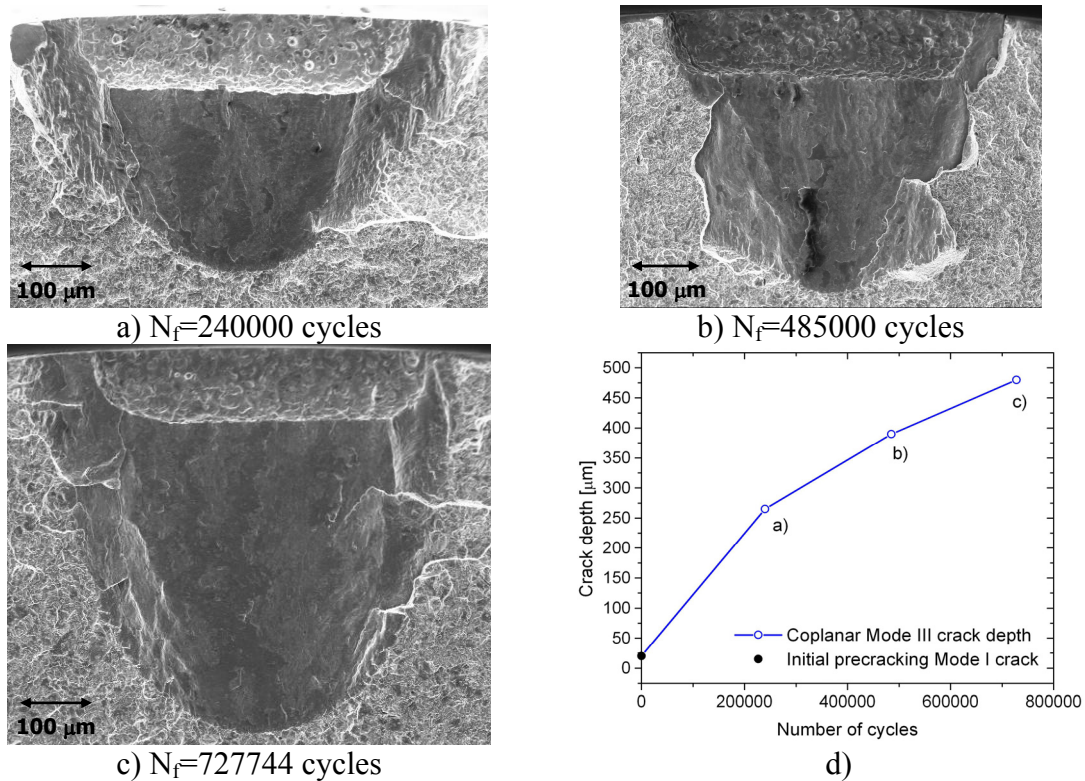


Figure 8. Mode III co-planar propagation rate for micronotch $\sqrt{\text{area}}=221.2 \mu\text{m}$, during the out-of-phase multiaxial test, a), b), c), fractography of tests interrupted at different number of cycle showing crack depths 265, 390, 480μm; d) co-planar crack growth

Results of these test set shows decreasing tendency within increasing of the co-planar crack depth, (see Fig.8d). FE analysis are being carried out in order to correlate crack shape evolution and growth rate with friction [8].

DISCUSSION AND REMARKS

Short Crack Effect in Mode III Under Torsion

The summary of the torsional tests clearly shows a definite ‘short crack effect’ for the Mode III propagation (Fig.9).

The conclusion that $\Delta K_{th,III}$ is approximately equal to the Mode I threshold is in accordance to similar results obtained by Murakami [9] for a annealed 0.47%carbon steel (JIS S45C). Also the onset of stable co-planar growth shows a definite size dependence.

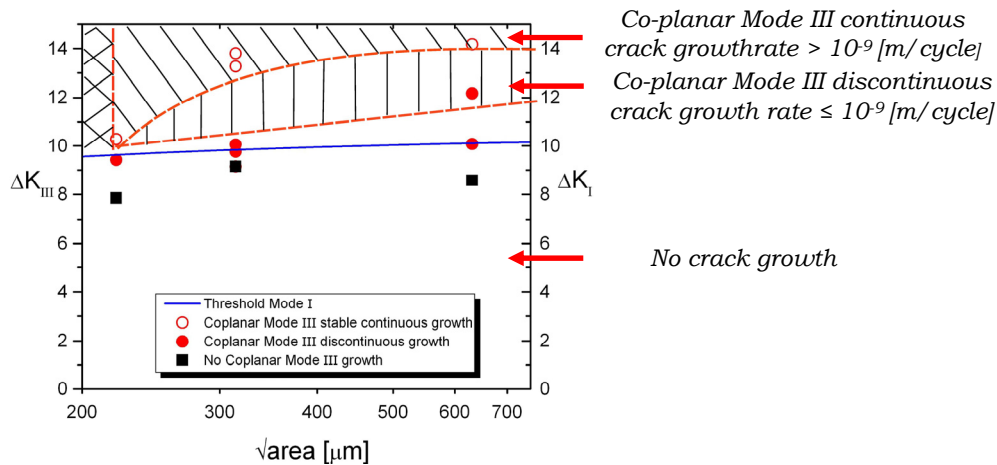


Figure 9. Comparison of the torsion fatigue tests results with Mode I threshold

Effect of Multiaxiality

The effect of test type in terms of Mode III co-planar crack growth rate and of Mode III stress intensity factors is showed in the Fig.10, for a defect with $\sqrt{\text{area}}=314.5 \mu\text{m}$.

In Fig.10.b it is possible to see effect the test type onto the value of minimum ΔK_{III} that is able to promote discontinuous co-planar crack growth.

For the in-phase mutiaxial fatigue test, at least at the stress ratio $R=-1$ and at the applied ratio between Mode III and Mode I, the conclusion that $\Delta K_{th,III} \approx \Delta K_{th,I}$ seems to be conformed in agreement with the torsional fatigue test results. In contrary the out-of-phase multiaxial fatigue tests results, at the same ratio between Mode III and Mode I, show e reduction of the the minimum ΔK_{III} above which there is nucleation of the co-planar growth respect to the torsional tests.

Analysis of the fatigue test results in terms of co-planar discontinuous crack growth rates gives some confusing result (see Fig.10.a): adopting the hypotethese, that during the Mode III crack growth friction and interlocking of the crack surfaces has vital influence of the growth rates, it is possible to explain the increase of the crack growth rate for the in-phase loading scheme, comparing with ones for torsional loading considering a deacresed friction on crack faces [10]. On the other hand, for out-of-phase loading, some other effect should be present (see for example Doquet [4]).

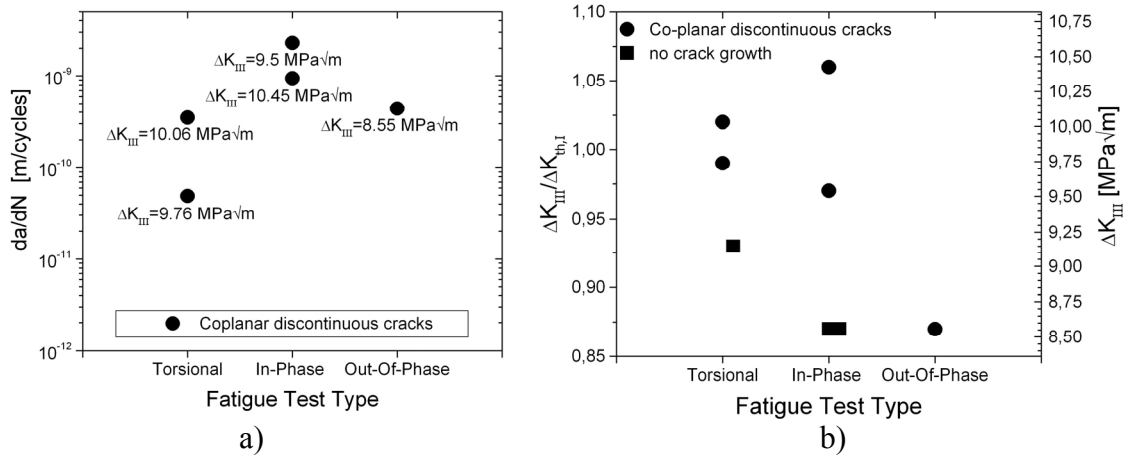


Figure 10. Comparison of the effect of test type onto a defects with $\sqrt{\text{area}} = 314.5 \mu\text{m}$
a) propagation rate; b) ΔK_{III} minimum for discontinuous growth vs fatigue test type

Stability of Co-planar Growth Under Out-Of-Phase Tests

The comparison between the out-of-phase fatigue tests shows the effect of the superimposed cyclic compressive stress. Increasing the maximum compressive stress in agreement with the real state of stress in rolling contact fatigue condition (specimen O.2 and O.3), the stable co-planar crack growth is promoted since Mode I propagation on a tilted planes appears to be less rapid. This behaviour could be explained by means of estimation of the stress intensity factors for the tilted plane experimentally observed at the bottom of the micro notches ($\theta = 45^\circ$ in Fig.7).

Considering the bottom of the micro notches, where K_{II} is approximately equal to zero, and the plane at $\varphi = 0$, the near-field solution for the stress distribution at the crack front, in a cylindrical coordinate system with the coordinates r , φ , and z , can be simplified in the following way [11]:

$$\begin{cases} \sigma_r = \sigma_\varphi = \frac{K_I}{\sqrt{2\pi r}}; & \sigma_z = \nu(\sigma_r + \sigma_\varphi) = \frac{2\nu K_I}{\sqrt{2\pi r}} \\ \tau_{r\varphi} = \tau_{rz} = 0; & \tau_{\varphi z} = \frac{K_{III}}{\sqrt{2\pi r}} \end{cases} \quad (2)$$

where the parameters K_I , K_{II} and K_{III} are the initial (main) crack stress intensity factors for the three fracture modes.

Resolving the stress state in Eq.2 onto a tilted plane, identified by an angle θ , it is possible to obtain the tensile stress and the shear stress near the tip of a tilt crack and the corresponding Mode I and Mode III tilt crack stress intensity factors:

$$\begin{cases} k_I = \frac{K_I}{2}(1+2\nu) + \frac{K_I}{2}\cos(2\theta)(1-2\nu) - K_{III}\sin(2\theta) \\ k_{III} = \frac{K_I}{2}\sin(2\theta)(1-2\nu) + K_{III}\cos(2\theta) \end{cases} \quad (3)$$

The results, see Fig.11 and Tab.3, show a very high negative value of the stress ratio R (specimen O.2 and O.3), that leads to the vanishing of Mode I propagation with an average Mode I growth rate more than two times less than Mode III one. Delaying in this way Mode I cracks, this type of multiaxial loading favours faster stable Mode III crack growth.

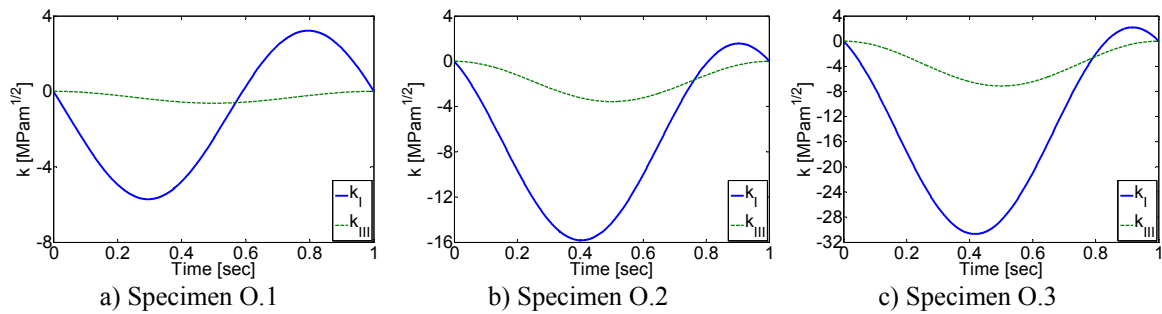


Figure 11. Mode I and Mode III tilt crack stress intensity factors in out-of-phase multiaxial tests ($\theta=45^\circ$ tilted plane)

Finally, the competition of failure modes under torsional and out of phase loading can be summarized as shown in Fig.12, where a schematic representation of the crack growth rate in Mode I + III is reported for both cases for defect with $\sqrt{\text{area}}=221.2 \mu\text{m}$. Looking at torsional fatigue test results it's possible to conclude that the formation of co-planar Mode III growth appears for ΔK_{III} values near $\Delta K_{I,th}$. Increasing this value ($\Delta K_{III} = 1.08 \Delta K_{I,th}$) the co-planar crack growth became more stable but the specimen failed in Mode I lead to the conclusion that at these ΔK_{III} levels Mode I growth is faster than Mode III (see Fig.12a). On the contrary, a superimposed axial compressive stress in an out-of-phase multiaxial fatigue test seems to completely change the previously observed behavior.

Table 3. Mode I stress intensity factors on tilted planes in out-of-phase multiaxial tests.

Specimen №	Micro notch $\sqrt{\text{area}}$ [μm]	$\Delta K_{I,45^\circ}$ [$\text{MPa}\sqrt{\text{m}}$]	$R_{I,45^\circ}$	$K_{I,max45^\circ}$ [$\text{MPa}\sqrt{\text{m}}$]	Average growth rate [m/cycles]	
					Surface crack	Mode III
O.1	314.5	8.93	-1.78	3.22	$2.51 \cdot 10^{-9}$	$4.43 \cdot 10^{-10}$
O.2	221.2	17.30	-10.16	1.56	$2.23 \cdot 10^{-10}$	$6.60 \cdot 10^{-10}$
O.3	631	32.86	-14.08	2.18	$4.71 \cdot 10^{-9}$	$1.07 \cdot 10^{-8}$

Applying the same ΔK_{III} value the co-planar crack growth is again stable (with an average rate close to the one observed in the torsional tests), but the surface crack growth is much more slow (see Fig.12b).

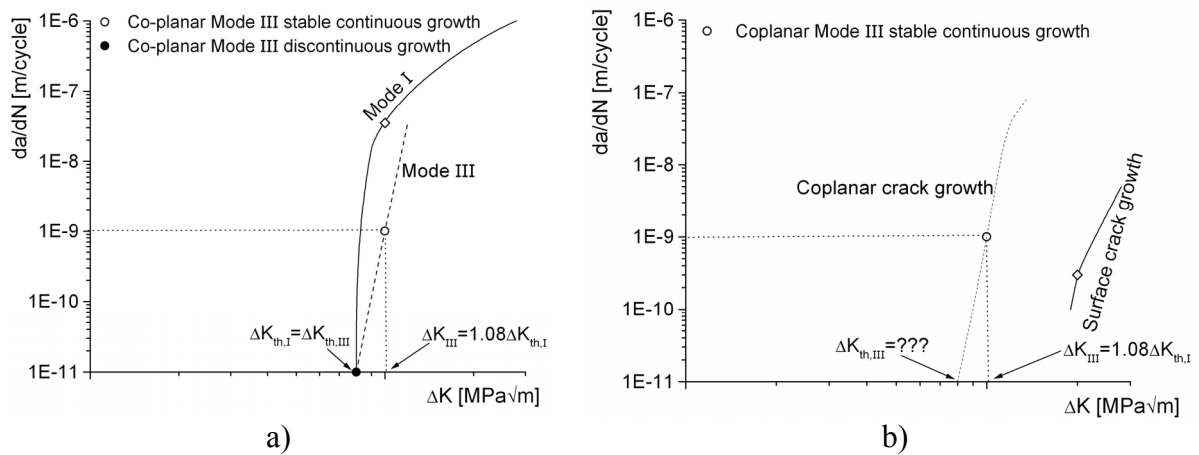


Figure 12. Schematic crack propagation rates for micronotch $\sqrt{\text{area}}=221.2 \mu\text{m}$: a) torsional test, b) multiaxial out-of-phase test.

CONCLUSIONS

The conclusions that can be drawn from the present results (further in-phase and out-of-phase tests are being carried out) onto gear SAE5135 steel are:

- there is a definite ‘short crack effect’ in Mode III both for the onset of Mode III growth and the ΔK_{III} at which crack growth becomes stable (for defects with $\sqrt{\text{area}} < 1000 \mu\text{m}$ the threshold $\Delta K_{th,III}$ values are quite close to Mode I in accordance to [8]) and for the ΔK_{III} needed for a growth rate $da/dN > 10^{-9}$ m/cycle;
- stable co-planar Mode III growth in torsional tests is also observable at ΔK_{III} levels at which Mode III growth is much less rapid than Mode I (contrary to the observations by Tschegg [12]);
- out-of-phase loading leads to a reduction of the minimum ΔK_{III} above which there is the initiation of co-planar growth respect to torsional tests;
- out-of-phase multiaxial loading, under stress levels corresponding to conditions of rolling contact fatigue, promotes stable co-planar Mode III growth since mixed-mode propagation on other propagation planes appears to be less rapid.

ACKNOWLEDGMENTS

The authors acknowledges the financial support by TENARIS Dalmine for this research activity. The Ph.D. scholarship of Khaydar Valiullin was also supported by TENARIS Dalmine.

REFERENCES

1. Murakami, Y. and Endo, M., *Int. J. Fatigue*, Vol. 16, 1994, pp. 163-181.
2. Murakami, Y., Takahashi, K., Kusumoto, R., *Fat. Fract. Engng. Mater. Struct.*, Vol. 28, 2004, pp. 49-60.
3. Nalla, R.K., Campbell, JP., Ritchie, R.O., *Int. J. Fatigue*, Vol. 24, 2002, pp. 1047-1062.
4. Doquet, V. and Pommier S., *Fat. Fract. Engng. Mater. Struct.*, Vol. 27, 2004, pp. 1051-1060.
5. Beretta, S., Valiullin, K., Proc. *European Conference on Fracture*, ESIS, Brno, 2008.
6. Pook, L.P., *Crack Paths*, WitPress, Southampton, UK, 2002.
7. K.L. Johnson, *Contact Mechanics*, Cambridge University Press, Cambridge, 1985.
8. Murakami, Y., Kaneta, M., *ASME*, Vol.113 April 1991, pp. 270-275.
9. Murakami, Y., Takahashi, K., Toyama, K., *ATEM'03, JSME-MMD.*, Sep. 10-12, 2003.
10. E.K. Tschegg, S.E. Stanzl, H.R. Mayer, M. Czegley, *Fat. Fract. Engng. Mater. Struct.*, Vol. 16, 1992, pp. 73-83.
11. Richard H.A., Fulland M., and Sander M., *Fat. Fract. Engng. Mater. Struct.*, Vol. 28, 2005, pp. 3-12.
12. E.K. Tschegg, S.E. Stanzl, *ASTM STP 924*, Vol.1 1988, pp. 214-232